Structural features and electronic properties of group-III-, group-IV-, and group-V-doped Si nanocrystallites

2007 J. Phys.: Condens. Matter 19 466211

(http://iopscience.iop.org/0953-8984/19/46/466211)

IOP PUBLISHING JOURNAL OF PHYSICS: CONDENSED MATTER

J. Phys.: Condens. Matter **19** (2007) 466211 (12pp) doi:10.1088/0953-8984/19/46/466211

Structural features and electronic properties of group-III-, group-IV-, and group-V-doped Si nanocrystallites

L E Ramos[1], Elena Degoli[2], G Cantele[3], Stefano Ossicini[2], D Ninno[3], J Furthmüller[1] and F Bechstedt[1]

[1] Institut für Festkörpertheorie und -optik, Friedrich-Schiller-Universität Jena and the European Theoretical Spectroscopy Facility (ETSF), Max-Wien-Platz 1, D-07743 Jena, Germany
[2] CNR-INFM-S[3] and Dipartimento di Scienze e Metodi dell'Ingegneria, Università di Modena e Reggio Emilia, via Amendola 2, Padiglione Morselli, I-42100 Reggio Emilia, Italy
[3] Coherentia CNR-INFM and Università di Napoli 'Federico II'—Dipartimento di Scienze Fisiche, Complesso Universitario Monte S. Angelo, Via Cintia, I-80126 Napoli, Italy

E-mail: lramos@ifto.physik.uni-jena.de

Received 17 April 2007, in final form 4 October 2007
Published 25 October 2007
Online at stacks.iop.org/JPhysCM/19/466211

Abstract

We investigate the incorporation of group-III (B and Al), group-IV (C and Ge), and group-V (N and P) impurities in Si nanocrystallites. The structural features and electronic properties of doped Si nanocrystallites, which are faceted or spherical-like, are studied by means of an *ab initio* pseudopotential method including spin polarization. Jahn–Teller distortions occur in the neighborhood of the impurity sites and the bond lengths show a dependence on size and shape of the nanocrystallites. We find that the acceptor (group-III) and donor (group-V) levels become deep as the nanocrystallites become small. The energy difference between the spin-up and spin-down levels of group-III and group-V impurities decreases as the size of the Si nanocrystallite increases and tends to the value calculated for Si bulk. Doping with carbon introduces an impurity-related level in the energy gap of the Si nanocrystallites.

(Some figures in this article are in colour only in the electronic version)

1. Introduction

The quantum confinement properties of silicon nanocrystallites (NCs) and similar nanostructures have been intensively investigated in recent years due to the promising applications of these structures in new electronic devices [1–3]. Due to the fact that electrons and holes experience a strong spatial localization in Si NCs, the radiative recombination rates increase in comparison with Si bulk. There are reports on optical gain in Si NCs [4], and new

devices have been suggested recently [5, 6]. Besides applications in data storage devices, basic research on NCs could lead to Si-based optoelectronic devices whose main advantage is to be compatible with the Si technology.

Since the early investigations on Si NCs, the influence of the NC size on its electronic properties is well known and supported by measurements [7, 8]. Nanocrystallites have a molecule-like energy-level spectra with dispersionless energy levels. The energetic separation between the lowest unoccupied molecular orbital (LUMO) and highest occupied molecular orbital (HOMO), that is the energy gap, is controlled primarily by the size of the particle. Surface treatments with solutions, different passivation of the dangling bonds or oxidation of the Si NC are other factors known to be important for the electronic properties of these materials [8–13]. On the other hand, the shape of the NCs can influence the luminescence efficiency, since the changes in their internal electric fields tend to separate electrons and holes spatially [14]. Less clear is the influence of doping on the electronic properties observed in porous Si (pSi) composed by Si NCs of different sizes. Doping of Si NCs is expected to introduce additional levels close to the HOMO or LUMO in the same fashion as it does for Si bulk. The detection of slight changes in the electronic levels in the neighborhood of the HOMO and LUMO of Si NCs are possible with the recent experimental techniques [15]. In addition to this, some experiments show that the concentration of carriers in Si NCs is influenced by quantum confinement [16]. An enhancement of the absorption in the infrared region of the spectra was observed when porous Si is doped with phosphorus, showing that the electronic structure is substantially modified by doping [17, 18]. Heavy doping of Si NCs with boron and boron–phosphorus co-doping was investigated recently, as well as the effects of doping on the photoluminescence (PL) peaks and crystal growth [19–23].

While the doping of Si NCs with boron and phosphorus was investigated in detail, the doping with group-IV species and other group-III and group-V species have not yet been investigated experimentally. Only one experiment on the role of nitrogen in the formation of Si NCs is reported in the literature [24]. *Ab initio* theoretical investigations on doping of Si NCs comprehend many impurities, being carried out initially for aluminum [25, 26] and phosphorus [25–28], and then for other group-III and group-V species in Si NCs. On the other hand, the previous investigations have been restricted to small NCs [28–31]. Localized surface modifications, such as a single termination of a different atomic species, which is not hydrogen, show significant effects on the electronic properties of Si NCs [32], though the effects are reduced in the presence of oxide covering shells [33]. Since doping is a fundamental process in semiconductor technology, and size and shape can alter the electronic properties of Si NCs, the knowledge of impurity levels in different NCs can be crucial for the development of devices.

We present an investigation of doped Si NCs, concerning their electronic structure and the influence of the shape and size on the incorporation of impurities. Our results intend to serve as guide to interpret measurements in Si NCs, where group-III, group-IV, and group-V impurities are intentionally present or not. A description of the approximations and theoretical methods employed is given in section 2. In section 3, we present the results for structural relaxation, electronic structure, defect levels, and formation energies of doped Si NCs. A summary and conclusions follow in section 4.

2. Methods

The total energies and eigenvalues are calculated by the independent-particle Kohn–Sham scheme within the framework of the density-functional theory (DFT) and generalized-gradient approximation (GGA) [34], as they are implemented in the Vienna *Ab Initio* Simulation Package [35, 36]. In the case of doping with group-III and group-V impurities we perform

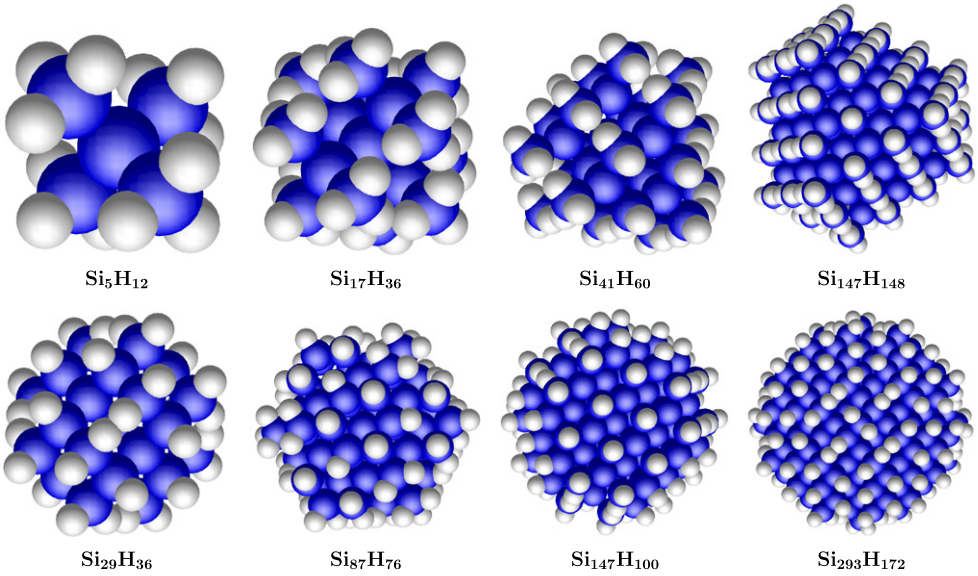

Figure 1. Faceted (top) and spherical-like (bottom) undoped Si NCs. The dark spheres represent the Si atoms and the light spheres represent the H atoms.

spin-polarized calculations, since in this case the NCs have an odd number of electrons. Pseudopotentials model the interaction between valence electrons and atomic nuclei [37]. Such pseudopotentials require a low energy cut-off for plane waves in comparison with norm-conserving pseudopotentials and are suitable for the calculation of optical matrix elements. An energy cut-off of 16 Ryd suffices to achieve convergence of the atomic forces. We perform an optimization of the atomic positions of doped and undoped Si NCs, which minimizes the interatomic forces on each atom to less than 20 meV $Å^{-1}$. To evaluate the effects of Jahn–Teller distortions on the minimization of the total energies, we perform ionic relaxation without any symmetry constraint.

The Si NCs are modeled by using the supercell method and by means of simple-cubic supercells whose size varies with the diameter of the NC. More than 15 Å of vacuum separate points at the surface of the NC and its images in the supercell method. The large size of the supercells justifies the restriction of the **k**-point sampling in the Brillouin zone to the Γ point. The dangling bonds at the surface of the Si NCs are passivated with H atoms, which excludes the possible effects of surface states and surface reconstructions from our investigation. Although Si NCs usually experience oxidation, there are experiments where the dangling bonds at the surface are passivated with H [7, 38, 39]. According to previous investigations on the localization of the HOMO and LUMO of Si NCs passivated with H, these states are not related to H atoms [40–42]. Therefore, the changes in the HOMO–LUMO gap of the Si NCs refer to quantum confinement effects and to the levels that may be introduced by the substitutional impurities considered. Concerning the shape of the NCs, we consider both spherical-like and faceted Si NCs. The spherical-like NCs are obtained by cutting Si atoms outside a sphere from Si bulk [40], whereas the faceted NCs result from a shell-by-shell construction procedure, in which one starts from a central atom and adds shells of atoms successively [33, 42, 43]. In figure 1 the spherical-like Si NCs and their average radii r are the clusters $Si_{29}H_{36}$ ($r = 5.4$ Å), $Si_{87}H_{76}$ ($r = 7.8$ Å), $Si_{147}H_{100}$ ($r = 9.3$ Å), and $Si_{293}H_{172}$

($r = 11.5$ Å) and the faceted Si NCs are the clusters Si_5H_{12} ($r = 3.2$ Å), $Si_{17}H_{36}$ ($r = 4.7$ Å), $Si_{41}H_{60}$ ($r = 6.3$ Å), and $Si_{147}H_{148}$ ($r = 9.4$ Å). Due to its small size the Si_5H_{12} NC could be classified either as spherical-like or as faceted. The atomic sites of the Si NCs at their initial configuration resemble locally the ones of the diamond structure (T_d point symmetry), where the atoms have a tetrahedral coordination. In both spherical-like and faceted Si NCs, there is a Si atom at the center. In the following, we consider the average radius of the Si NCs as the average distance of the H atoms with respect to the center of the Si NC. The substitutional impurity site is localized at the center of the NC. By taking into account only one impurity in the Si NCs we study a wide range of doping concentrations, which vary approximately from 2×10^{20} cm^{-3} (1 mol%) to 7×10^{21} cm^{-3} (20 mol%). We compare bond lengths, formation energies, and spin splittings of the doped Si NCs with those of Si bulk doped with the same substitutional impurities. In this case, the calculations are performed in simple-cubic supercells containing 215 Si atoms and a substitutional impurity atom.

In order to quantify the position of the impurity-related levels and perform an energy alignment for the electronic density of states of the undoped and doped Si NCs, an energy reference ε_H analogous to the top of the valence band in Si bulk and the HOMO in Si NCs should be determined. In practice, the energy reference of the doped Si NC does not necessarily coincide with the one of the undoped Si NC. However, the average electrostatic potential at the vacuum region is constant for both doped and undoped Si NCs. We use the difference of the absolute values of the potentials in at the vacuum region to perform the energy alignment of the two systems and shift the density of states and the whole energy spectra according to this energy [44, 45]. The position of ε_H in the doped system is calculated following the procedure described above as well [44, 45].

For the group-III (B and Al), group-IV (C and Ge), and group-V (N and P) impurities, we calculate the formation energies by $\Omega_f[X] = E_{tot}[X] - E_{tot} + \mu_{Si} - \mu_X$, where $E_{tot}[X]$ (X = B, Al, C, Ge, N, and P) is the total energy of the doped Si NC, E_{tot} is the total energy of the undoped Si NC, and μ_{Si} and μ_X are the chemical potentials of the reservoirs for the Si and for the X species, respectively.

3. Results

3.1. Structural features

After ionic relaxation under no symmetry constraint, the first neighbors of the impurity in the Si NCs experience different displacements. In figure 2 we show the Si–X bond lengths (X = B, Al, C, Ge, N, and P) of the four nearest neighbors to the impurity versus the total number of Si atoms in the nanocrystallite.

Except for the B and Al impurities, there is a general trend to a decrease of the Si–X bond length as the size of the Si NC decreases. The differences of bond lengths due to the shape of the Si NCs are remarkable. As a rule, the Si–X bond lengths of faceted Si NCs are longer than the ones for the spherical-like Si NCs, even when they have similar average radii. One of the four first nearest neighbors of the B impurity is displaced differently from the other three neighbors, indicating a trend for the relaxation under C_{3v} symmetry. Although the Si–N bond lengths also show a tendency for relaxation under C_{3v} symmetry, the differences among the bond lengths are not as large as Si–B bond lengths. On the other hand, the Si–Al bond lengths do not suggest a particular symmetry lowering due to ionic relaxation. This is in accordance with our theoretical predictions for the expansion of the Si–Si bonds at the center of the Si NCs [40, 42, 43]. We verify that this trend is not modified if the central atom of the Si NC is replaced by an impurity atom. Zhou and co-workers also report an expansion of the Si–Si

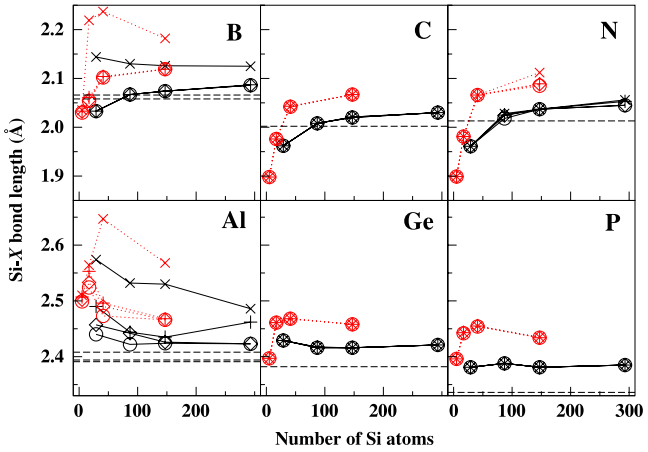

Figure 2. Silicon–X bond lengths (X = B, Al, C, Ge, N, and P) for the spherical-like (solid lines) and faceted doped Si NCs (dotted lines) versus the number of Si atoms. The four Si–X bond lengths are indicated by circles, diamonds, plus signs, and crosses, and are connected with straight lines to guide the eyes. The dashed lines indicate the values of the silicon–X bond lengths for the X substitutional impurity in bulk.

bonds for Si NCs doped with group-V impurities [30]. The Si–X bond lengths in the doped Si NCs are usually longer than those in Si bulk for the impurities which have a similar or larger covalent radius than Si (Al, Ge, and P). This happens due to the expansion of the Si–Si bonds observed at the center of the Si NCs [40, 42, 43]. For impurities with small covalent radii in comparison with Si and for small Si NCs, there is less constraint for the ionic relaxation and the Si–X bond lengths can be shorter than the ones in bulk.

3.2. Impurity formation energies

The energetic stability of the impurities in the Si NCs is quantified by their formation energies described in section 2. An estimate of the chemical potentials for the reservoirs of the different atomic species is made by performing calculations either for a diatomic molecule or for a crystalline phase of the atomic species. Following this procedure, the chemical potential of the nitrogen reservoir is taken as the cohesive energy of the N_2 molecule divided by two, $\mu_N = -8.12$ eV. Estimates of chemical potentials of C, Si, and Ge are obtained from a diamond structure leading to $\mu_{Si} = -5.41$ eV, $\mu_C = -8.90$ eV, and $\mu_{Ge} = -4.52$ eV, respectively. For Al the chemical potential $\mu_{Al} = -3.67$ eV was obtained from its face-centered cubic structure. The chemical potential $\mu_B = -6.40$ eV for the B reservoir is obtained from one of the most common structures for B, known as T-50 (space group $P4_2/nnm$). We suppose a reservoir of black phosphorus to make an estimate of the chemical potential of the phosphorus reservoir $\mu_P = -5.29$ eV. Although other crystalline phases are also suitable to model the reservoirs, the differences of the procedures to calculate the chemical potentials only result in a rigid shift of the formation energies, which is common to all the Si NCs doped with the same impurity.

The influence of shape and size of the NCs on the impurity formation energies is shown in figure 3 for doped Si NCs versus their reciprocal radii. The formation energies of Ge and P impurities depend mainly on the size of the particle and have an almost linear dependence on the reciprocal radius of the Si NC. While the formation energy of the first-row elements C and N may increase for large Si NCs, the formation energy of B, Al, and P decreases. This fact is related to the lattice deformation that large atoms can cause in small Si NCs when incorporated

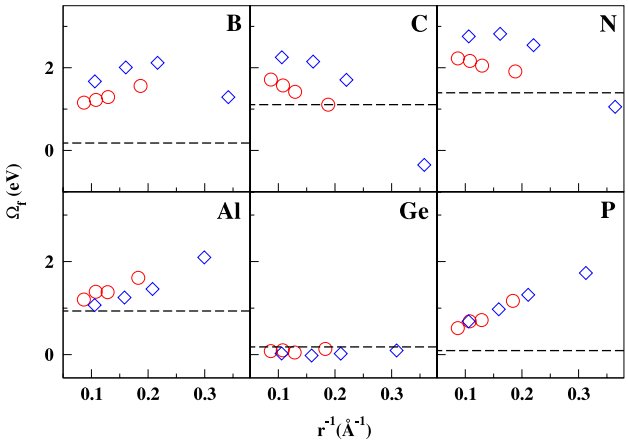

Figure 3. Impurity formation energies of B, Al, C, Ge, N, and P versus the reciprocal radii of the doped Si NCs. The energy values are given for faceted (diamonds) and spherical-like (circles) doped Si NCs. The dashed lines indicate the impurity formation energies in Si bulk.

in a substitutional site. The smaller the Si NC, the larger is the deformation caused by the impurity. Since B leads to symmetry lowering as Al does and large deformation as P does, the impurity formation energies of B are high in small Si NCs. Only the formation energy of the Ge impurity is nearly independent of the size of the nanocrystallite. This fact is related to the similar chemical properties of Si and Ge. A comparison between faceted and spherical-like NCs shows that the incorporation of the impurity in Si NCs is more favorable if the NC has facets in the case of Al, is nearly shape-independent for Ge and P, and costs more energy for the other impurities considered. Except for Ge and the C and N doping of the smallest Si NCs, the impurity formation energies of the Si NCs are higher than in Si bulk. This can be explained in terms of longer Si–X bond lengths and the symmetry lowering of the doped Si NCs, which require additional relaxation of the atomic positions in comparison with Si bulk.

3.3. Electronic structure

3.3.1. Kohn–Sham defect levels. It has been verified by calculating the lowest electron–hole pair excitation energies that a partial cancelation of quasiparticle and excitonic effects occurs, at least for the sizes of NCs considered [40, 42, 43, 46–49]. The cancelation of these effects implies that a good estimate of the HOMO–LUMO energy gap can already be obtained from the differences of Kohn–Sham eigenvalues calculated within the DFT and GGA. Since electronic levels of undoped Si NCs, such as the HOMO and the LUMO, and the impurity levels exhibit similar localization, the DFT and GGA can be fair approximations for the position of those levels.

It is known that some properties of Si NCs, such as the HOMO–LUMO gap, can be described by a function proportional to $r^{-\alpha}$, where r is the average radius of the particle and α is a real number typically close to 1.0 [46]. In figure 4 the position of the Kohn–Sham impurity levels in the energy-gap region as well as the HOMO–LUMO gap of the undoped Si NCs shows nearly a linear dependence versus the reciprocal radii of the NCs. An increase of quantum confinement, which means a decrease of the NC size, leads to deep impurity levels in the doped Si NCs. In Si NCs the B and Al impurities induce shallow acceptor levels, whereas the N and P impurities induce deep and shallow donor levels, respectively. Only small variations of the

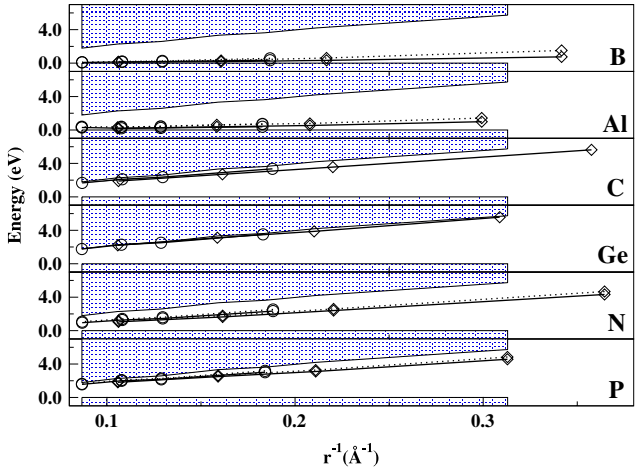

Figure 4. Energetic position of the Kohn–Sham impurity levels versus the reciprocal radii of the spherical-like (circles) and faceted (diamonds) Si NCs. The solid and dotted lines correspond to the spin-up and spin-down impurity levels. The HOMO of the undoped Si NCs coincides with ε_H of the doped Si NCs. For the C- and Ge-doped Si NCs, the position of the LUMO is shown instead of the impurity level.

HOMO–LUMO gaps due to the shape of the Si NCs can be perceived in figure 4 and do not vary significantly with the shape of the Si NCs. The fact that the positions of the KS impurity levels in figure 4 vary with size of the Si NC is important, since other properties of NCs such as the hyperfine splitting are found to have the same dependence on the size [17, 27].

The positions of the energy levels near the LUMO for the C- and Ge-doped Si NCs are shown in figure 4 and the partial charges of these states are in figure 5. The LUMOs of the C-doped Si NCs are clearly related to the carbon impurity. While the LUMO of C-doped Si NCs is concentrated at the center of the NC, the LUMO of Ge-doped Si NCs is as disperse as the other states near the HOMO and LUMO, indicating that it is particularly related to the Ge atom. The incorporation of C in Si NCs introduces an energy level at a lower energy than the LUMO of the corresponding undoped Si NC. This results in a narrowing of the HOMO–LUMO gap in C-doped Si NCs, in contrast to the Ge-doped Si NCs, where the gap remains practically unchanged. For the $Si_{87}H_{76}$ NC doped with N and P impurities, our results for the impurity levels are in qualitative agreement with the ones reported by Zhou and co-workers [30]. Small numerical differences between our results and the ones in [30], such as the HOMO–LUMO gap of the $Si_{87}H_{76}$ NC, arise from the different approaches and methods applied.

The incorporation of group-III and group-V impurities leads to an odd number of electrons, in contrast to the group-IV impurities, which do not alter the total number of electrons in the system. As a consequence, the impurity level with the lower energy (spin up or spin down) is occupied and the level with higher energy is not occupied. As shown in figure 4 the increasing of quantum confinement with the reduction of the NC size results in energy differences Δ_{spin} between the spin-up and spin-down impurity-related levels. It is interesting to note that the energy difference between spin-up and spin-down levels has the same order of magnitude as the Stokes shifts of undoped Si NCs [42]. In figure 6, the difference in energy between spin up and spin down is shown versus the NC radius. The value of Δ_{spin} depends slightly on the shape of the Si NC but it is mostly related to its size. For small Si NCs, the value of the splitting is larger for the group-III impurities than for the group V. The values of Δ_{spin} of Si NCs are always above the corresponding values in Si bulk.

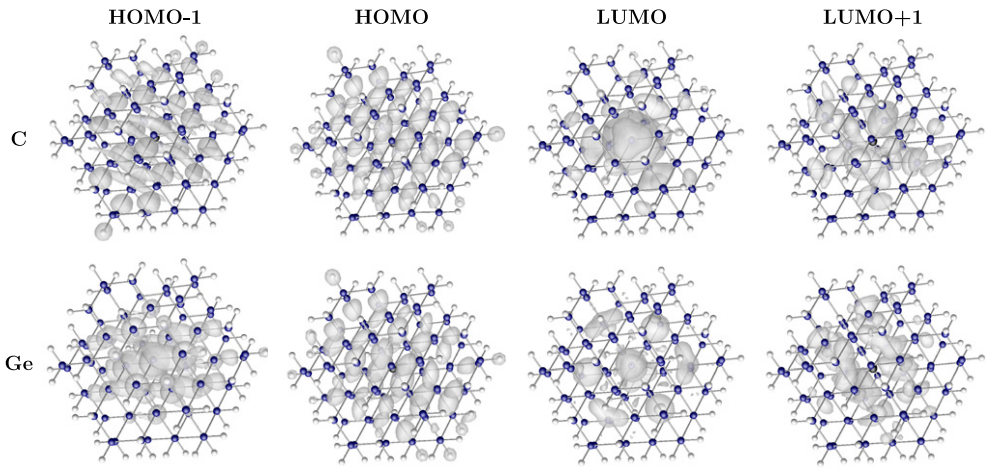

Figure 5. Representation of the atomic positions and of an isocharge surface of the HOMO, HOMO − 1, LUMO and LUMO + 1 for a doped $Si_{87}H_{76}$ NC.

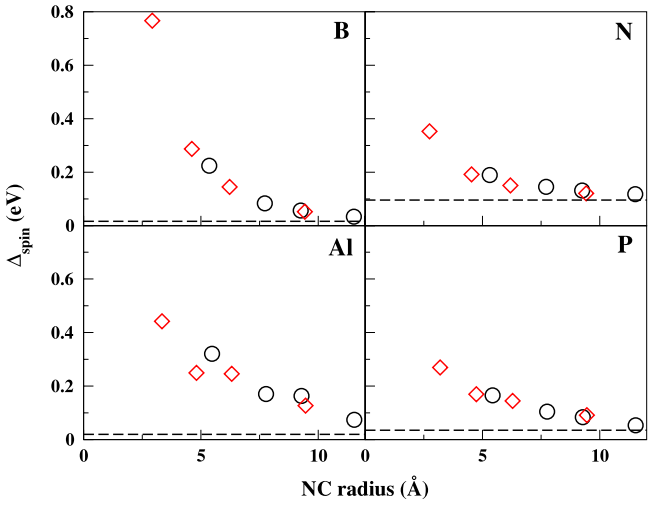

Figure 6. Differences in energy between the spin-up and spin-down impurity states (Δ_{spin}) versus the Si NC radius for faceted doped Si NCs (diamonds), spherical-like doped Si NCs (circles) and doped Si (dashed lines).

3.3.2. Boron and aluminum. The incorporation of the group-III impurities boron and aluminum in Si NCs results in a different number of spin-up and spin-down electrons. According to the density of states shown in figure 7, the group-III impurities introduce shallow acceptor levels in the gap that become shallower as the size of the Si NC increases. For small Si NCs a redistribution of states occurs at higher and lower energies than the energy-gap region and the energy difference of spin-up and spin-down levels is more pronounced. As the size of the Si NC increases, the energy difference between the spin-up and spin-down B and Al impurity levels becomes small. The occupied spin level of Al is very close in energy to other occupied levels, as indicated by the difference of peak heights of the spin-up and spin-down energy levels in figure 7.

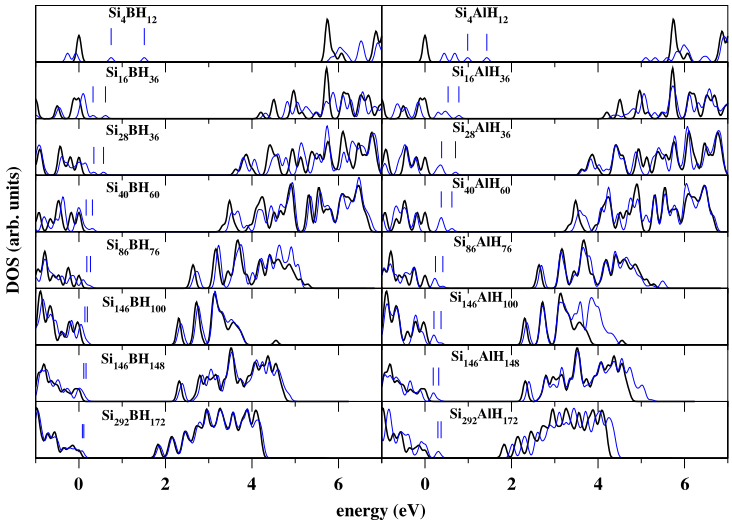

Figure 7. Electronic density of states of undoped Si NCs (thick solid lines) and Si NCs (thin solid lines) doped with group-III impurities. The energy zero is set to the value of ε_{H} for each system. The vertical lines indicate the position of the spin-up and spin-down impurity-related levels.

3.3.3. Carbon and germanium. As group-IV impurities, both carbon and germanium are isovalent to silicon and therefore impurity levels related to these impurities are expected, only if significant displacements of the atoms surrounding the impurities occur. As reported in previous investigations, the Si–Si bonds tend to be elongated at the center of the undoped Si NCs, whereas these bonds are slightly shortened near the surface of the NC [42, 43]. The short covalent radius of C in comparison to the covalent radius of Si induces displacements of the Si neighboring atoms towards the impurity site. This fact has some implications in the electronic states such as an energy shift of the electronic states close the HOMO and the LUMO with respect to the vacuum level of small C-doped Si NCs. In figure 4 we observe that the overall effect of the incorporation of C impurities is a slight narrowing of the HOMO–LUMO gap of the Si NCs. Since Ge is chemically similar to Si and has practically the same covalent radius, its incorporation at one site in Si NCs has less influence on electronic properties than C. On the other hand, interesting properties are predicted when several Ge atoms are incorporated either at the center or at the surface of Si NCs [42].

The electronic densities of states shown in figure 8 for the C- and Ge-doped Si NCs are compared with the DOS of the undoped Si NCs. Especially for large Si NCs, the main structure of the DOS peaks at energies above the HOMO and below the LUMO is maintained. The similarity between Si and Ge results in much less change in the DOS than for the C impurity. As in figure 4, some impurity-related peaks appear at positions below the LUMO, notably for the smallest doped Si NCs. In the case of Ge-doped Si NCs, the variation of the energy gap is negligible, though the position of the levels with respect to the vacuum level can change, especially in small Si NCs.

3.3.4. Nitrogen and phosphorus. The reduced size of the N atom in comparison with P results in important differences between these two dopants. In figure 9, the peaks in the DOSs for Si NCs doped with group-V impurities show a similar structure out of the energy range of the HOMO–LUMO gap. As for the group-III and group-IV impurities, the redistribution and

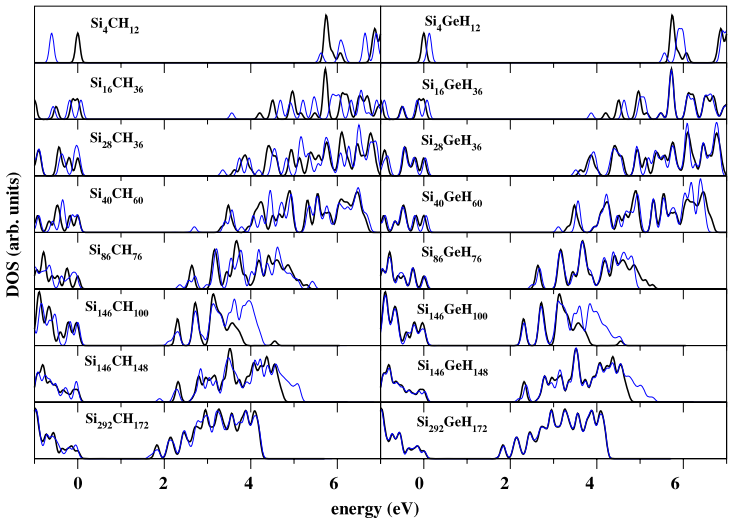

Figure 8. Electronic density of states of undoped Si NCs (thick solid lines) and Si NCs doped with group-IV impurities (thin solid line).

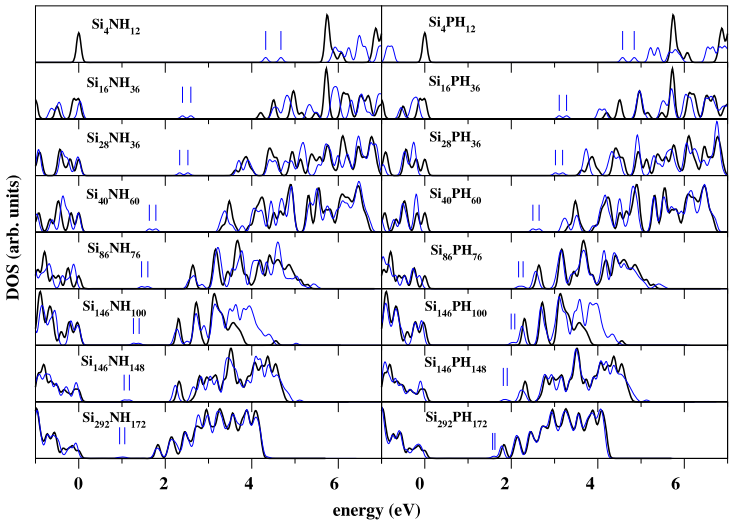

Figure 9. Electronic density of states of undoped (thick solid lines) Si NCs and Si NCs doped with group-V impurities (thin solid lines). The energy zero is set to the value of ε_{H} for each system. The vertical lines indicate the positions of the spin-up and spin-down impurity-related levels.

shift of energy states, due to the doping, is more visible for small doped Si NCs than for the large ones. While N induces a mid-gap donor level in Si NCs, the impurity level induced by P is clearly a shallow donor. One remarkable difference of N with respect to the group-III and group-IV impurities, and also to the P impurity, is that its impurity level does not become shallow when the size of the Si NC increases. This is important in view of the fact that often light-emitting Si NCs are obtained from thermally induced nucleation in amorphous Si-rich nitride films [50].

4. Summary and conclusions

By means of an *ab initio* pseudopotential method and taking into account spin polarization, we studied the effects of size and shape on the bond lengths, formation energies, electronic impurity levels and density of states of Si NCs doped with group-III, group-IV, and group-V substitutional impurities. After ionic relaxation, the Si–X bond lengths (X = B, Al, C, Ge, N, and P) tend to be longer for faceted than for spherical-like Si NCs. For the largest doped Si NCs considered, the Si–X bond lengths are longer than for the corresponding impurity in Si bulk. A little variation of the KS impurity levels and HOMO–LUMO gaps with respect to the shape of the Si NCs is observed. Boron and aluminum give rise to shallow acceptor levels, whereas phosphorus gives rise to a shallow donor level and nitrogen to a deep donor level. The impurity levels become deeper as the size of the Si NC decreases. The calculated formation energies suggest that the incorporation of the impurities is more favored in spherical than in faceted Si NCs. This tendency is not valid for the Ge and P impurities, which have a formation energy nearly independent of the shape, and for the Al impurity whose incorporation is slightly more favored in faceted Si NCs. According to our calculations, the incorporation of B, Al and P impurities tends to be more favored energetically in the largest Si NCs. In comparison with the formation energies of the impurities in Si bulk most of the formation energies are higher, excepting the energy for Ge, that is similar for bulk and Si NCs. Large Si NCs doped with group-III and group-V impurities present a small energy difference between the spin-up and spin-down impurity energy levels. The value of this energy difference approaches the one calculated for the same impurity in Si bulk as the size of the Si NC increases, although it is always higher. This fact can be important for the optical absorption and emission in doped Si NCs.

Acknowledgments

The authors would like to thank the European Commission in the NANOQUANTA network of excellence (contract No NMP4-CT-2004-500198) and the Austrian *Fonds zur Förderung der wissenschaftlichen Forschung* (project No F25, *Nanostrukturen für Infrarot-Photonik*) for financial support. We acknowledge also the support of the MIUR PRIN (2005) Italy, of the CNR-CNISM 'Progetto Innesco', and of the CRUI Vigoni Project (2005–2006) Italy–Germany. The calculations were performed at the John von Neumann Institute for Computing (NIC) in Jülich, Germany (grant No HJN21/2006).

References

[1] Cullis A G, Canham L T and Calcott P D J 1997 *J. Appl. Phys.* **82** 909
[2] Bisi O, Ossicini S and Pavesi L 2000 *Surf. Sci. Rep.* **38** 1
[3] Ossicini S, Pavesi L and Priolo F 2003 *Light Emitting Silicon for Microphotonics* (*Springer Tracts in Modern Physics* vol 194) (Berlin: Springer)
[4] Pavesi L, Dal Negro L, Mazzoleni C, Franzò G and Priolo F 2000 *Nature* **408** 440
[5] Linnros J 2005 *Nat. Mater.* **4** 117
[6] Walters R J, Bourianoff G I and Atwater H A 2005 *Nat. Mater.* **4** 143
[7] Furukawa S and Miyasato T 1988 *Phys. Rev.* B **38** 5726
[8] Schuppler S, Friedman S L, Marcus M A, Adler D L, Xie Y-H, Ross F M, Chabal Y J, Harris T D, Brus L E, Brown W L, Chaban E E, Szajowski P F, Christman S B and Citrin P H 1995 *Phys. Rev.* B **52** 4910
[9] Seals L, Gole J L, Tse L A and Hesketh P J 2002 *J. Appl. Phys.* **91** 2519
[10] Gole J L, DeVincentis J A, Seals L, Lillihei P, Prokes S M and Dixon D A 2000 *Phys. Rev.* B **61** 5615
[11] Prokes S M, Carlos W E, Seals L and Gole J L 2000 *Phys. Rev.* B **62** 1878
[12] Wolkin M V, Jorne J, Fauchet P M, Allan G and Delerue C 1999 *Phys. Rev. Lett.* **82** 197

[13] Seraphin A A, Werwa E and Kolenbrander K D 1997 *J. Mater. Res.* **12** 3386
[14] Stoneham A M and McKinnon B A 1998 *J. Phys.: Condens. Matter* **10** 7665
[15] Pawlak B J, Gregorkiewicz T, Ammerlaan C A J, Takkenberg W, Tichelaar F D and Alkemade P F A 2001 *Phys. Rev.* B **64** 115308
[16] Timoshenko V Y, Dittrich T, Lysenko V, Lisachenko M G and Koch F 2001 *Phys. Rev.* B **64** 085314
[17] Fujii M, Mimura A, Hayashi S, Yamamoto Y and Murakami K 2002 *Phys. Rev. Lett.* **89** 206805
[18] Mimura A, Fujii M, Hayashi S, Kovalev D and Koch F 2000 *Phys. Rev.* B **62** 12625
[19] Boarino L, Geobaldo F, Borini S, Rossi A M, Rivolo P, Rocchia M, Garrone E and Amato G 2001 *Phys. Rev.* B **64** 205308
[20] Chen H and Shen W Z 2004 *J. Appl. Phys.* **96** 1024
[21] Fujii M, Toshikiyo K, Takase Y, Yamaguchi Y and Hayashi S 2003 *J. Appl. Phys.* **94** 1990
[22] Wensheng W, Tianmin W, Chunxi Z, Guohua L, Hexiang H and Kun D 2004 *Vacuum* **74** 69
[23] Fujii M, Yamaguchi Y, Takase Y, Ninomiya K and Hayashi S 2004 *Appl. Phys. Lett.* **85** 1158
[24] Mulloni V, Bellutti P and Vanzetti L 2005 *Surf. Sci.* **585** 137
[25] Zhou Z, Friesner R A and Brus L 2003 *J. Am. Chem. Soc.* **125** 15599
[26] Blomquist T and Kirczenow G 2004 *Nano Lett.* **4** 2251
[27] Melnikov D V and Chelikowsky J R 2002 *Phys. Rev. Lett.* **92** 046802
[28] Cantele G, Degoli E, Luppi E, Magri R, Ninno D, Iadonisi G and Ossicini S 2005 *Phys. Rev.* B **72** 113303
[29] Majumder C and Kulshreshtha S K 2004 *Phys. Rev.* B **70** 245426
[30] Zhou Z, Steigerwald M L, Friesner R A, Brus L and Hybertsen M S 2005 *Phys. Rev.* B **71** 245308
[31] Ossicini S, Degoli E, Iori F, Luppi E, Magri R, Cantele G, Trani F and Ninno D 2005 *Appl. Phys. Lett.* **87** 173120
[32] Puzder A, Williamson A J, Grossman J C and Galli G 2002 *J. Chem. Phys.* **117** 6721
[33] Ramos L E, Furthmüller J and Bechstedt F 2005 *Phys. Rev.* B **71** 035328
[34] Wang Y and Perdew J P 1991 *Phys. Rev.* B **44** 13298
[35] Kresse G and Furthmüller J 1996 *Comput. Mater. Sci.* **6** 15
[36] Kresse G and Furthmüller J 1996 *Phys. Rev.* B **54** 11169
[37] Kresse G and Joubert D 1999 *Phys. Rev.* B **59** 1758
[38] Takeoka S, Minoru F and Hayashi S 2000 *Phys. Rev.* B **62** 16820
[39] Wang Y Q, Smirani R and Ross G G 2004 *Nano Lett.* **4** 2041
[40] Degoli E, Cantele G, Luppi E, Magri R, Ninno D, Bisi O and Ossicini S 2004 *Phys. Rev.* B **69** 155411
[41] Luppi M and Ossicini S 2005 *Phys. Rev.* B **71** 035340
[42] Ramos L E, Furthmüller J and Bechstedt F 2005 *Phys. Rev.* B **72** 045351
[43] Ramos L E, Furthmüller J and Bechstedt F 2004 *Phys. Rev.* B **70** 033311
[44] Pöykkö S, Puska M J and Nieminen R M 1996 *Phys. Rev.* B **53** 3813
[45] García A and Northrup J E 1995 *Phys. Rev. Lett.* **74** 1131
[46] Proot J P, Delerue C and Allan G 1992 *Appl. Phys. Lett.* **61** 1948
[47] Delerue C, Lannoo M and Allan G 2000 *Phys. Rev. Lett.* **84** 2457
[48] Porter A R, Towler M D and Needs R J 2001 *Phys. Rev.* B **64** 035320
[49] Luppi E, Degoli E, Cantele G, Ossicini S, Magri R, Ninno D, Bisi O, Pulci O, Onida G, Gatti M, Incze A and Del Sole R 2005 *Opt. Mater.* **27** 1008
[50] Dal Negro L, Yi J H, Michel J, Kimerling L C, Hamel S, Williamson A and Galli G 2006 *IEEE J. Sel. Top. Quantum Electron.* **12** 1628